Changes in molecular dynamics upon formation of a polymer dispersed liquid crystal

Ana R. E. Brás,[1] M. Teresa Viciosa,[1] Carla M. Rodrigues,[1] C. J. Dias,[2] and Madalena Dionísio[1,*]
[1]*REQUIMTE, Departamento de Química, Faculdade de Ciências e Tecnologia da Universidade Nova de Lisboa, 2829-516 Caparica, Portugal*
[2]*Departamento de Ciências dos Materiais—CENIMAT, Faculdade de Ciências e Tecnologia da Universidade Nova de Lisboa, 2829-516 Caparica, Portugal*

(Received 6 October 2005; revised manuscript received 13 January 2006; published 22 June 2006)

The molecular dynamics during the formation of a polymer dispersed liquid crystal (PDLC) was followed by dielectric relaxation spectroscopy in the frequency range from 10^{-1} to 2×10^{6} Hz and over the temperature range from 158 to 273 K. The composite was produced by thermal polymerization induced phase separation of a mixture of triethyleneglycol dimethacrylate and the nematic liquid crystal, E7, in the proportion of 60:40 w/w. Both monomer and liquid crystal vitrify upon cooling having glass transition relaxation processes already characterized by some of us; yet E7 was previously studied in a narrower frequency range, so the present work updates its dielectric behavior. The starting mixture exhibits a rather complex dielectric spectrum due to the detection of multiple processes occurring simultaneously in the monomer and liquid crystal constituents. The PDLC formation occurs by mobility changes essentially in the liquid crystal tumbling motion, while the main relaxation of the monomer depletes upon polymerization. A low intense secondary process of E7 hardly detected in the bulk material is enhanced in both starting mixture and final composite allowing its characterization.

DOI: 10.1103/PhysRevE.73.061709 PACS number(s): 61.30.Pq, 77.22.Gm, 64.70.Pf

I. INTRODUCTION

Polymer dispersed liquid crystals (PDLC) consist of nematic liquid crystal droplets dispersed in a polymer host, which are able to switch electrically from an opaque scattering state to a highly transparent state, having potential for a wide range of electro-optical applications [1–5].

PDLCs are usually prepared by a polymerization induced phase separation process (PIPS), being the assessment of its performance in most applications, intimately related to the morphologies emerging under polymerization [6]. The dynamical evolution during the formation of a PDLC is determined by the simultaneous crosslinking polymerization of the monomer and segregation of liquid crystal that coexist, at intermediate times, with unreacted monomer. Dielectric relaxation spectroscopy may provide here useful information since it monitors the molecular mobility through the reorientation of molecular dipoles under the influence of an oscillating electrical field. It also contributes to the understanding of the orientation of the liquid crystal under an electrical field which plays a major role in the PDLCs performance and is not well understood at a molecular level [7].

In the present work we investigated, by dielectric relaxation spectroscopy, the formation of a PDLC having 3-ethyleneglycol-dimethacrylate (TrEGDMA)/E7 (60:40) w/w as starting mixture, where the TrEGDMA polymerization was induced by the 2,2′-azo-bis-isobutyronitrile (AIBN) initiator according to a free radical mechanism; since TrEGDMA monomer is bifunctional, the final product has a crosslinked structure, belonging to a class of multifunctional acrylate monomers widely used in the production of coatings, information storage systems, spherical lenses and dental biomaterials [8–10].

Both TrEGDMA and E7, a nematic liquid crystalline mixture, easily supercool having calorimetric glass transition temperatures of 187 [11] and 211 K respectively [12,13]. The nematic temperature range of E7 is thus greatly extended relative to single liquid crystals, extending from its nematic to isotropic transition at 313 K down to the glass transition temperature. The relaxation processes associated with the glass transition of both bulk monomer and E7 were already dielectrically characterized by some of us [11,14]. Besides the main glass transition relaxation process that diminishes under polymerization, TrEGDMA also exhibits a secondary relaxation related with localized mobility, which stays over after polymerization reaches completion [15]. The E7 nematic mixture presents the dielectric behavior of a single component unaligned liquid crystal, where the dipole moment relaxes complementary between parallel (more intense process in bulk material) and perpendicular alignments relative to the applied electrical field, presenting simultaneously the typical features found in oriented samples [14]. Therefore, the E7 [14] dielectric spectra reveal a superposition of two relaxation mechanisms: a main relaxation peak involving the hindered rotation about the short molecular axis, related to the parallel alignment of the director in the electric field (frequently designated as delta process) and high frequency process originated by librational fluctuations around the long molecular axis, related to the perpendicular alignment of the director in the electric field. Additionally, a third relaxation process was detected at low frequencies, that was attributed to either reorientation motion of molecular aggregates [16,17], or partially immobilized molecules [18]. The perpendicular contribution and the low frequency process manifest as, respectively, high and a low frequency shoulders largely merged under the main peak. E7 is now

*Corresponding author. Electronic address: madalena.dionisio@dq.fct.unl.pt

studied in an enlarged frequency and temperature range allowing a better resolution.

In the present work, dielectric spectra were collected for the precursor mixture and at different conversion degrees until full monomer conversion. The spectra present a rather complex profile owing to the simultaneous detection of multiple processes originated by each composite constituent. The changes in different relaxation processes during the PDLC formation were analyzed through activation and isochronal plots and compared with bulk materials.

The present work is a contribution to understand the molecular dynamical evolution during the formation of such composites, which, to our knowledge, was never reported in literature. So far most of the dielectric studies concern with bulk low molecular weight LCs [19–22], liquid crystalline polymers [19,23–26] and final form PDLC [14,27–30].

The dielectric study of the liquid crystal orientation dispersed on the polymer matrix will also allow the investigation of the Maxwell-Wagner-Sillars (MWS) effect originated by the coexistence of two different dielectric media that screens the influence of the applied electrical field, affecting the electro-optical response. The investigation of both aspects, (a) molecular dynamic evolution and (b) orientation of liquid crystal, will allow tailoring materials with high performance in practical applications.

II. EXPERIMENTAL

The 3-ethylene glycol dimethacrylate monomer, TrEGDMA, with the formula

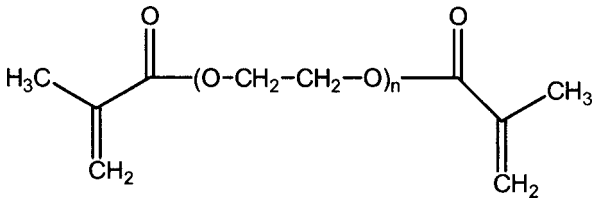

with $n=3$ and $M_w=286.36$, was supplied by Fluka, catalog No. 90412.

The monomer was previously passed through a disposable inhibitor remover column from Aldrich, Ref. 306312-1EA, in order to eliminate the hydroquinone stabilizer. The polymerization initiator was AIBN from Aldrich, Catalog No. 11630, being used in the proportion 0.1% w/w relative to TrEGDMA. The nematic liquid crystalline mixture E7, with the following composition [31,32]: 4-cyano-4′-pentyl-1,1′-biphenyl (51%), 4-*n*-heptyl-4′-cianobiphenyl (25%), 4,4′-*n*-octyloxycyanobiphenyl (16%) and 4′-*n*-pentyl-4-cyanoterphenyl (8%) w/w, was supplied by Merck KGaA (Darmstadt, Germany). The composition of the studied mixture was TrEGDMA/E7 60:40 w/w.

III. DIFFERENTIAL SCANNING CALORIMETRY

A SETARAM DSC 131 calorimeter fitted with a liquid nitrogen cooling accessory was used for the differential scanning calorimetry measurements. Dry high purity N_2 gas was purged trough the sample during the measurements. Samples were cooled down to −120 °C and the thermograms collected in the subsequent heating run at 5 K/min.

A. Dielectric relaxation spectroscopy

The dielectric measurements were carried out using a broadband impedance analyzer, Alpha-N analyzer from Novocontrol GmbH, covering a frequency range from 10^{-1} Hz to 2 MHz. A drop of the TrEGDMA/E7 mixture with two silica spacers 50 μm thick was placed between two gold plated electrodes (diameter 20 mm) of a parallel plate capacitor. The sample cell (BDS 1200) was mounted on a cryostat (BDS 1100) and exposed to a heated gas stream being evaporated from a liquid nitrogen dewar. The temperature control was performed within ±0.5 °C, with the Quatro Cryosystem. Novocontrol GmbH supplied all these modules.

Dielectric spectra were collected for bulk liquid crystal from −115 to 0 °C in increasing temperature steps: in the temperature range $-115\ ^\circ\mathrm{C} \leqslant T \leqslant -30\ ^\circ\mathrm{C}$, the dielectric spectra were recorded every 2 °C; in the remaining temperature region the spectra were recorded every 5 °C.

For the precursor mixture, dielectric spectra were collected in increasing temperature steps from −115 up to 25 °C: in the temperature range $-115\ ^\circ\mathrm{C} \leqslant T \leqslant 0\ ^\circ\mathrm{C}$, the dielectric spectra were recorded every 2 °C; in the remaining temperature region the spectra were recorded every 5 °C.

To induce different polymerization degrees, the TrEGDMA/E7 mixture was kept at 70 °C during three periods of time $t_{\min}$, according to the following procedure:

Path 1—heating of the mixture from 0 up to 70 °C;

Path 2—the mixture is kept isothermally at T_{pol} during $t_{\min}$; $t_{\min}$ was, respectively, 15, 30, 150 min;

Path 3—cooling the mixture down to −115 °C; and

Path 4—acquisition of the dielectric spectra of the TrEGDMA/E7 mixture partially polymerized from −115 up to 0 in the same temperature steps as the precursor mixture.

In order to reach full polymerization [15], the mixture was further heated to 120 °C in increasing steps of 10 °C, by maintaining it 10 min at each temperature, cooled down to −115 °C and remeasured (according to path 4).

B. The data treatment

The real and imaginary parts of the complex dielectric constant $[\varepsilon^*(\omega)=\varepsilon'(\omega)-i\varepsilon''(\omega)]$ were fitted by a sum of the well-known Havriliak-Negami (HN) function [33]

$$\varepsilon^* = \varepsilon_\infty + \sum_j \frac{\Delta\varepsilon_j}{[1+(i\omega\tau_j)^{\alpha_{\mathrm{HN}_j}}]^{\beta_{\mathrm{HN}_j}}}, \tag{1}$$

where j is the number of relaxation processes; $\Delta\varepsilon$ is the dielectric strength, τ is the characteristic relaxation time, related to the frequency of the maximum of the loss peak $\tau \approx (2\pi f_{\max})^{-1}$, and α_{HN} and β_{HN}, the shape parameters $(0<\alpha_{\mathrm{HN}}<1,\ 0<\alpha_{\mathrm{HN}}\beta_{\mathrm{HN}}<1)$. At the highest temperatures, data are influenced by low frequency conductivity contribution, and an additional term $i(\sigma/\omega\varepsilon_0)$ was added, where ε_0 is the vacuum permittivity, and σ is the dc conductivity of the sample. Furthermore, in some spectra, a MWS process was

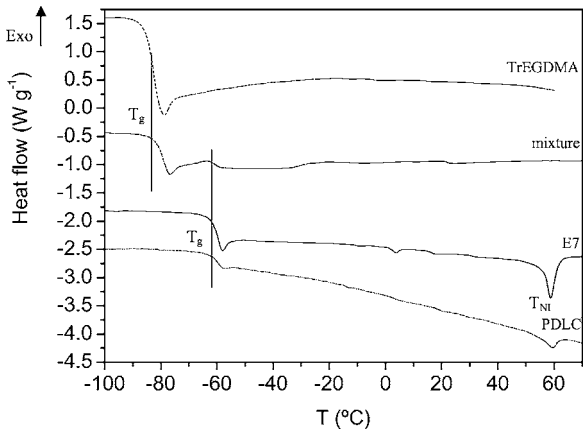

FIG. 1. DSC thermograms for bulk constituents, precursor mixture and PDLC composite, taken in heating mode at 5 K/min; curves were vertically displaced for better comparison.

detected that was taking in account in the fitting procedure as an additional HN process.

The curvature affecting the temperature dependence of the relaxation times of cooperative processes obeys the Volger-Fulcher-Tamman (VFT) law [34–36]

$$\tau = \tau_0 \exp^{B/(T-T_0)}. \tag{2}$$

The replacement of the activation energy equation $E_a = R(d \ln \tau)/(d1/T)$ in Eq. (2) allows the calculation of a temperature dependent activation energy

$$E_a(T) = \frac{R \,.\, B}{\left(1 - \frac{T_0}{T}\right)^2} \tag{3}$$

Finally, from $E_a(T)$ it is possible to estimate a fragility index according Angell's formula [37]

$$m = \frac{E_a(T_g)}{\ln 10 \,.\, R \,.\, T_g} \tag{4}$$

IV. RESULTS

A. Differential scanning calorimetry

Differential Scanning Calorimetry (DSC) runs were performed for both precursor and full polymerized mixtures in order to investigate the transition temperatures. Figure 1 shows the thermograms collected from −100 up to 70 °C at 5 K/min after a cooling path from room temperature down to −120 °C.

The DSC runs of neat constituents are included in Fig. 1 for comparison, evidencing their respective glass transitions (T_g). Additionally, E7 exhibits its nematic to isotropic transition (T_{NI}).

As can be seen, the thermogram for the precursor mixture presents two transitions at low temperatures that correspond to the glass transition of each mixture component, having a slight deviation (around 3 K) towards each other. The nematic to isotropic transition of E7 is absent in the initial mixture but is detected in the PDLC, as well as the E7 glass transition. The absence of TrEGDMA's glass transition in the full polymerized material confirms the monomer conversion. Moreover, the E7 transitions detected in the PDLC, i.e., when the liquid crystal is encapsulated within the polymer matrix, match with bulk E7. From the ΔC_p and ΔH_{NI} (in units of mass) associated respectively with the glass and nematic to isotropic transition of E7 incorporated in the PDLC, relatively to bulk E7, it is possible to estimate the fractional amount of E7 contained in LC domains through the equation proposed by Smith *et al.* [38]

$$\alpha = \frac{m_{\mathrm{LC}}^D}{m_{\mathrm{LC}}} = \left(1 + \frac{m_P}{m_{\mathrm{LC}}}\right) P(x), \tag{5}$$

where m_{LC}^D is the mass of LC which has phase separated from the polymer, m_{LC} and m_P are the masses, respectively, of LC and polymer in the PDLC, x is the LC concentration, and

$$P(x) = \frac{\Delta H_{\mathrm{NI}}(x)}{\Delta H_{\mathrm{NI}}(\mathrm{LC})} \; or \; P(x) = \frac{\Delta C_{p_{\mathrm{LC}}}(x)}{\Delta C_{p_{\mathrm{LC}}}(\mathrm{LC})} \tag{6}$$

represent the ratios of nematic-isotropic transition enthalpy or heat capacity increment for the PDLC to the equivalent value for bulk LC [$\Delta H_{\mathrm{NI}}(\mathrm{E7_{bulk}}) = 4.99$ J g^{-1} and $\Delta C_p(\mathrm{E7_{bulk}}) = 0.404$ J g^{-1} °C^{-1} here determined, in close agreement with Ref. [39], $\Delta H_{\mathrm{NI}}(\mathrm{E7_{PDLC}}) = 0.593$ J g^{-1} and $\Delta C_p(\mathrm{E7_{PDLC}}) = 0.119$ J g^{-1} °C^{-1}]. For the α estimation, m_p was calculated taking into account the monomer conversion degree determined by isothermal polymerization (the full thermal study will be published elsewhere). The estimated α (ΔH_{NI}) and α (ΔC_p) values are, respectively, 0.26 and 0.66, in accordance with the phase separated liquid crystal fraction determined for an acrylated/E7 based PDLC at the same composition [40], revealing that a significant liquid crystal amount is solubilized in the polymer matrix. The same type of calculation cannot be extrapolated for the precursor mixture, since Eq. (5) is strictly valid only if the segregated liquid crystal exhibits the same thermophysical behavior as in the bulk state [39]. This is not case, but the deviations in the glass transitions of both constituents confirm that some mutual solubility exists.

B. Dielectric relaxation spectroscopy

Due to the large amount of data we only fitted the data of precursor and full polymerized mixtures, comparing its behavior with the bulk materials. The mixtures at intermediate conversion degrees will help us to assign the various processes detected. The bulk materials will be briefly analyzed since the main results are already published.

1. Bulk E7

Figure 2(a) presents the three dimensional (3D) dielectric loss spectra of bulk unaligned E7 between −90 and −10 °C in logarithmic scale since data varies several orders of magnitude, enhancing simultaneously the secondary detected processes. As previously found [14], bulk E7 dielectric spectroscopy reveals a multiple process spectrum (see the Introduction) associated to the parallel and perpendicular

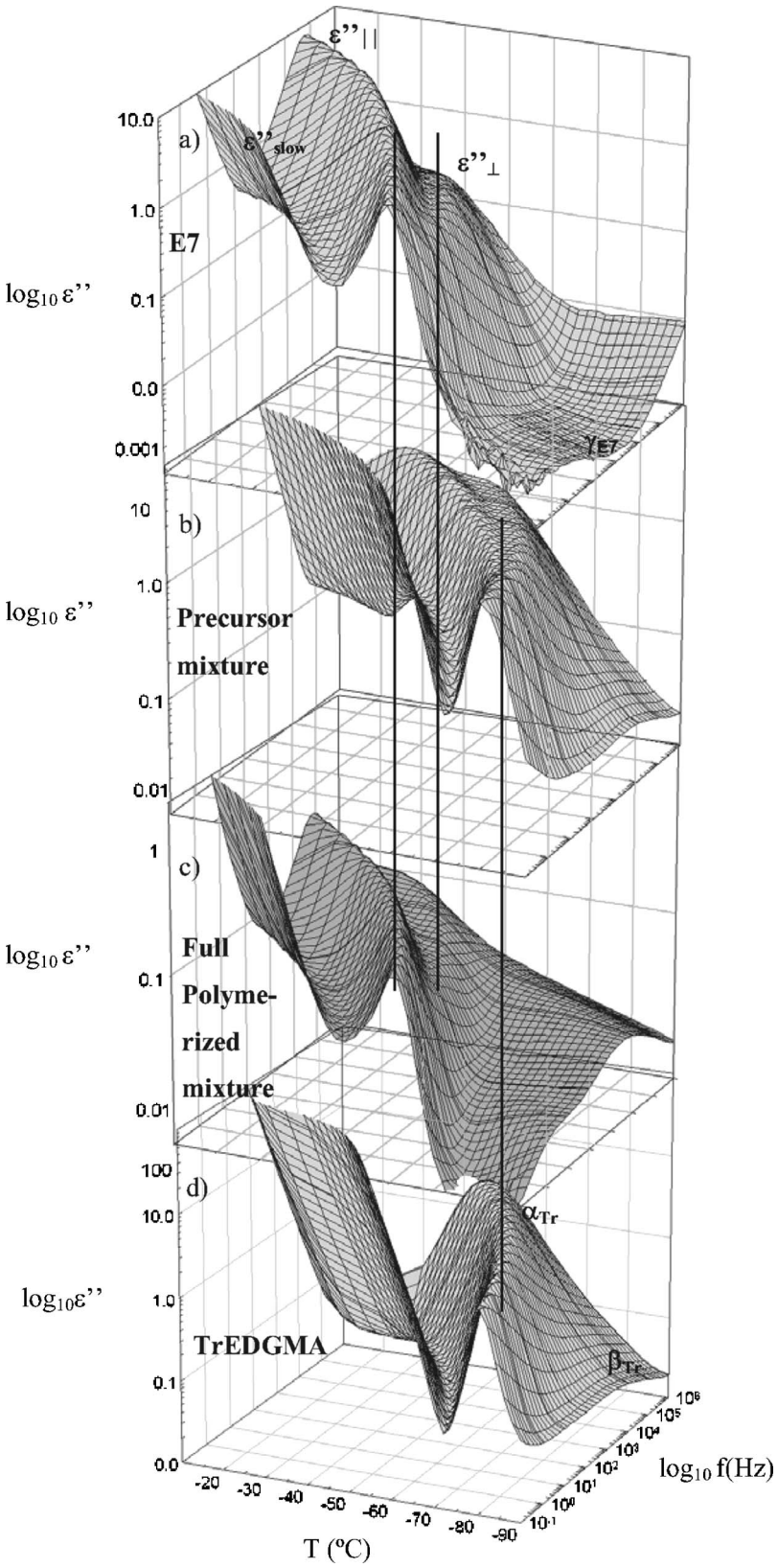

FIG. 2. 3D dielectric loss plots in logarithmic scale in the temperature range from −90 and −10 °C over the frequency range from 10^{-1} to 2×10^{6} Hz for (a) bulk E7, (b) precursor mixture, (c) full polymerized mixture, and (d) bulk TrEGDMA with 0.1% w/w AIBN (data taken from Ref. [15]); the individual relaxation processes of the pure constituents are identified. The vertical lines act as guide for the eyes to facilitate the assignment of the relaxation processes in the mixtures.

alignments of the nematic director [respectively, $\varepsilon_{\parallel}''$ and $\varepsilon_{\perp}''$ in Fig. 2(a)], the perpendicular component being better defined relatively to the previous published data. From the VFT fitting of the relaxation process associated with the short axis hindered rotations ($\varepsilon_{\parallel}''$) (data presented further on in Table I) the glass transition temperature was estimated by replacing $\tau=100$ s in Eq. (2) [41] as 207 K in close agreement with the calorimetric glass transition 211 K (Fig. 1) and as reported in Refs. [12,13]. From the activation energy value at T_g [Eq. (3)] a fragility index [Eq. (4)] of 74 was estimated.

TABLE I. Fitting shape parameters for all the detected relaxation processes and respective Arrhenian or VFT parameters obtained from the temperature dependence of the HN relaxation times (see Fig. 4). Included are the glass transition temperatures estimated from the VFT equation for $\tau=100$ s.

		Arrhenius		VFT					Fitting shape parameters	
		τ_0 (s)	E_a (kJ mol^{-1})	B (s)	T_0 (K)	τ_0 (s)	T_g (K) (τ=100s)	r^2	α	β
Precursor	α_{TrE}	-	-	1056±77	157.1±1.7	(1.0±0.5)×10^{-13}	188	0.998	0.89±0.04	0.45±0.06
	β_{TrE}	(3.6±0.9)×10^{-15}	37±1	-	-	-	-	0.999	0.61±0.06	0.32±0.02
	$\varepsilon''\|\|$	-	-	1082±892	169.1±22.7	(4.4±4.4)×10^{-12}	204	0.995	0.98±0.02	0.99±0.01
	$\varepsilon''\perp$	-	-	1166±71	152.6±1.8	(7.1±3)×10^{-13}	188	0.999	0.91±0.06	0.94±0.06
	γ	(1.8±1.2)×10^{-16}	51±2	-	-	-	-	0.994	0.46±0.03	0.95±0.05
Polymerized	α_{TrE}	-	-	-	-	-	-	-	-	-
	β_{TrE}	(1.1±0.1)×10^{-14}	36±1	-	-	-	-	0.999	0.45±0.05	0.46
	ε'' slow	-	-	393±92	194.9±4.2	(5.1±3.6)×10^{-7}		0.996	0.72±0.06	1.00
	$\varepsilon''\|\|$	-	-	1510±194	159.0±3.9	(7.2±5.6)×10^{-13}	205	0.998	0.83±0.06	0.6-1.0↑
	$\varepsilon''\perp$	-	-	1166±451	167.5±12.2	(1.7±1.1)×10^{-13}	201	0.995	0.83±0.06	0.53±0.10
	γ	(6.5±2.0)×10^{-15}	46±1	-	-	-	-	0.998	0.47±0.03	1.00
E7 bulk	ε''slow	-	-	1301±196	157.6±5.8	(2.6±1.8)×10^{-10}	206	0.998	0.64-0.95↑	0.86-0.65↓
	$\varepsilon''\|\|$	-	-	954±29	172.5±0.9	(6.8±1.4)×10^{-11}	207	0.999	1.00±0.00	1.00±0.00
	$\varepsilon''\perp$	-	-	387±49	195.1±1.6	(1.2±0.7)×10^{-10}	209	0.997	0.50-0.76↑	0.81±0.04
TrEGDMA[a]	α_{TrE}	-	-	1439±98	147±1.8	(1.9±1.1)×10^{-15}	185	0.995	0.95±0.02	0.47±0.01
	β_{TrE}	(2.1±1.2)×10^{-14}	35±1	-	-	-	-	0.997	0.42-0.48↑	0.49±0.02

[a] Data taken from Reference [15].

The slow process is noticeable between −56 and 0 °C [ε''_{slow} in Fig. 2(a)]. The enlarged frequency and temperature ranges of these measurements allowed the detection of a new process. This fourth process is observed at low frequencies in the temperature range of −90 and −80 °C (γ_{E7}; the γ notation was chosen in order to avoid confusion with a secondary process detected in TrEGDMA).

2. Bulk TrEGDMA

TrEGDMA was dielectrically characterized in Refs. [11,15]. Figure 2(d) presents the dielectric loss spectra in a 3D plot (ε'' in logarithmic scale) of TrEGDMA with 0.1% (w/w) of AIBN, where the main relaxation process associated with the glass transition (α_{Tr}) and the secondary process (β_{Tr}) are well separated. It was found that the initiator does not affect the dielectric spectra of pure TrEGDMA [15].

3. TrEGDMA/E7 mixture

Figures 2(b) and 2(c) display the 3D dielectric loss spectra of the 60:40 (w/w) TrEGDMA/E7 mixture, respectively, prior and after full polymerization (notice the different logarithmic ε'' scales). A multiple peak profile is observed owing to the superposition of different dielectric processes due to both monomer and liquid crystal. The assignment of individual processes will be accomplished along the text.

Figures 3(a)–3(c) (precursor) and Figs. 3(d)–3(f) (full polymerization) show the individual HN functions employed in the overall fit of the dielectric loss curves for, respectively, the precursor and the full polymerized mixture, detected at three different temperatures, respectively, −80, −60, and −42 °C showing all the detected processes; the insets show the fit of the corresponding real permittivity.

Figure 4 presents the relaxation times obtained from the fitting respectively for: (a) precursor mixture; (b) polymerized mixture. Both Figs. 4(a) and 4(b) include the relaxation times of bulk E7 and TrEGDMA monomer (filled gray symbols); data for TrEGDMA monomer was taken from Ref. [15].

Due to the large amount of adjustable parameters, the methodology employed in the fitting procedure was to start with the processes detected at the lowest temperatures and keep with small variations its shape parameters at higher temperatures when they are still detectable. In the precursor mixture, the first observed process was the β_{Tr} secondary relaxation of the monomer TrEGDMA followed immediately by the γ_{E7} process, only detected up to −90 °C [see Fig. 4(a)]. Since the secondary monomer process (β_{Tr}) was already well characterized [15] and the same shape parameters were found to apply in the actual spectra, the remaining γ_{E7} process was easily fitted in the lower temperature range. The entrance in the frequency window of the main relaxation process of TrEGDMA (α_{Tr}), above −90 °C, completely masks this γ_{E7} process. Consequently, at −80 °C [Figs. 3(a) and 4(a)] only β_{Tr} and α_{Tr} processes appear. Once again, the main relaxation process of the monomer maintain the same

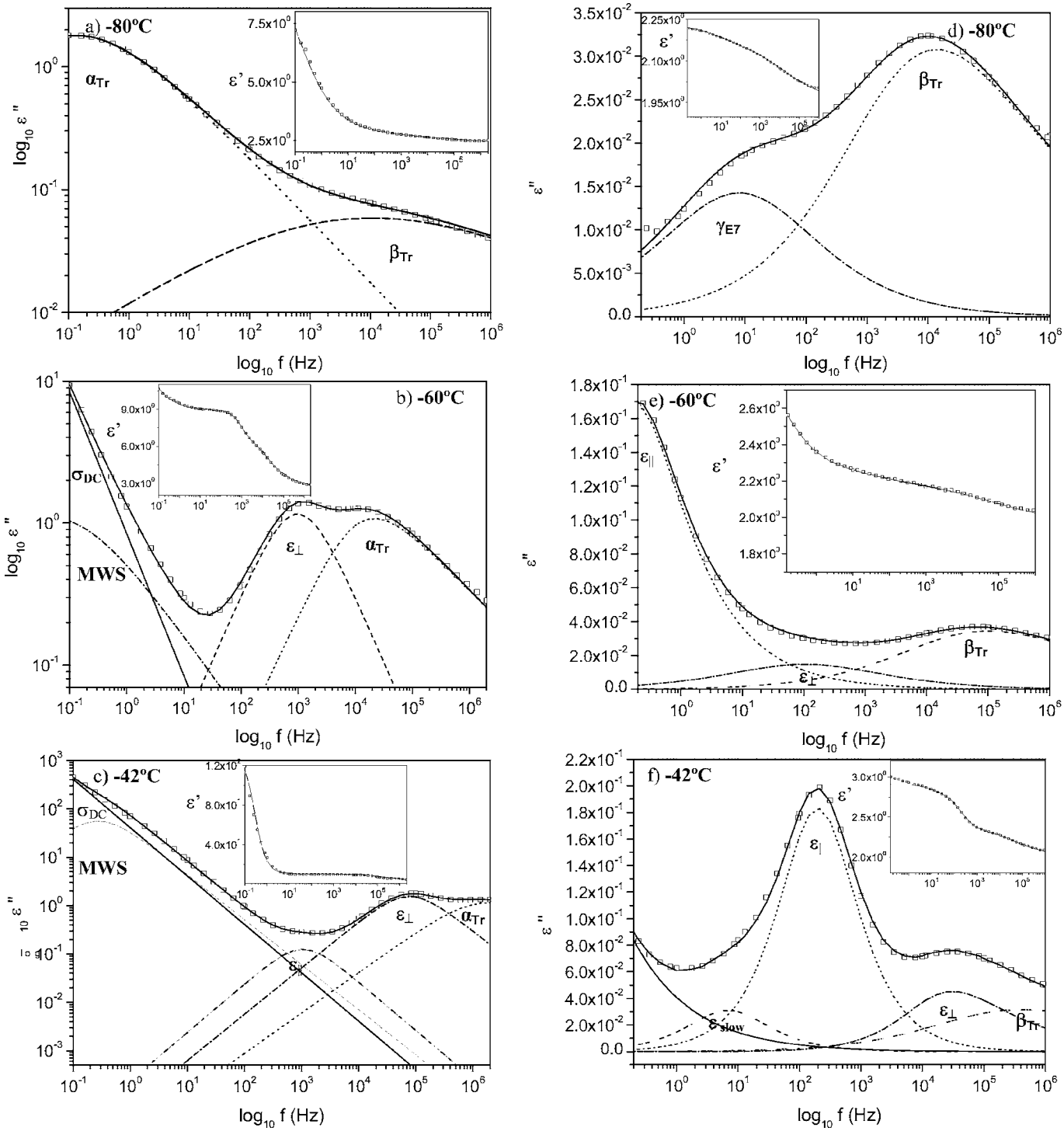

FIG. 3. Isothermal loss spectra showing the individual processes obtained by HN fittings for unreacted mixture [(a), (b), and (c)] and full polymerized [(d), (e), and (f)] at −80, −60, and −42 °C; for the unreacted mixture [(a)–(c)] the loss scale is logarithmic due to great intensity differences between detected processes. In the inset, the fitted (solid line) real part is shown.

shape parameters found in the fit of bulk TrEGDMA, so the overall fitting was easy to achieve through the optimization of the dielectric strength and relaxation time values. Above −80 °C, another relaxation process is observable partially superimposed to the α_{Tr} process. Given that is known that the monomer presents two relaxation processes, this new process certainly originates from E7. Figure 3(b), at −60 °C, shows the partial overlapping processes, and the individual HN curves. Finally in Fig. 3(c), at −42 °C, both the main relaxation of TrEGDMA and the relaxation originated by E7 are observed, together with a low intensity process.

Additionally, a MWS [42–44] process appears as a consequence of the coexistence of accumulation of charge at the interface of two media having different permittivities/

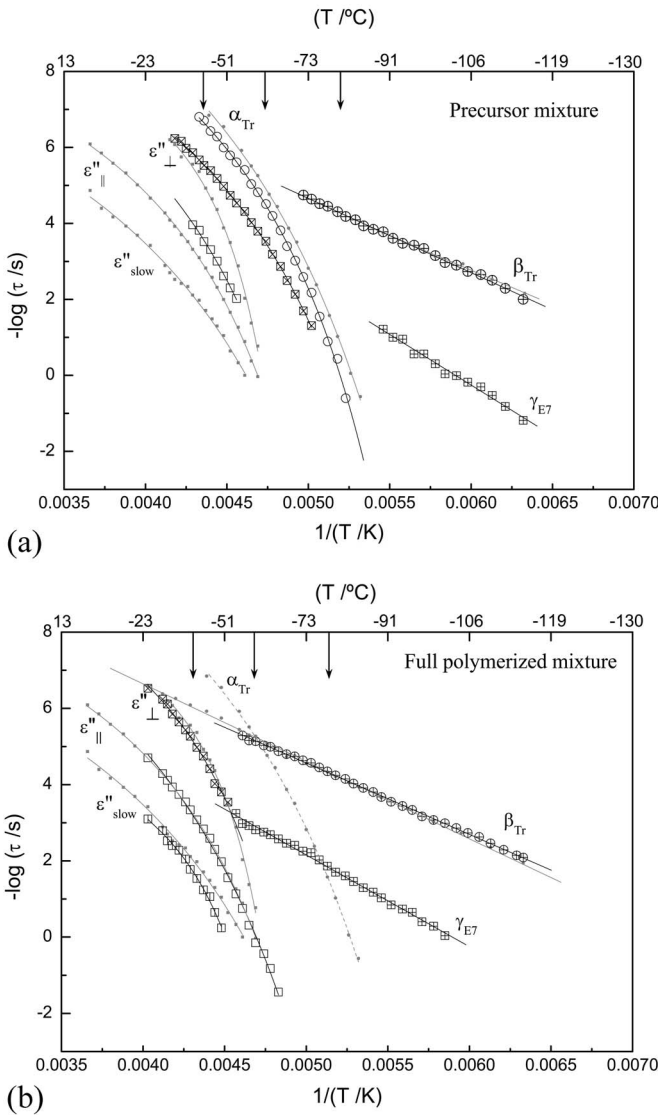

FIG. 4. Relaxation maps for all individual fitted processes detected in (a) precursor mixture and (b) full polymerized mixture; the time dependence for the relaxation processes detected in bulk materials is shown in filled gray symbols and identified in figure (a) (data taken from Ref. [15] for α_{Tr} and β_{Tr}); figure (b) identifies the processes detected in the polymerized mixture [same symbols in both figure (a) and (b)]; circles—TrEGDMA, squares—E7). The β_{Tr} filled gray circles with linear dependence in Fig. 4(b) corresponds to the secondary relaxation after full polymerization of bulk TrEGDMA with AIBN (0.1% w/w) (data taken from Ref. [15]). Solid lines are the respective Arrhenian and VFT fittings. The arrows correspond to the temperatures presented in Fig. 3.

conductivities, as the low frequency tail in the real permittivity demonstrates [insets of Figs. 3(b) and 3(c)]; also the term $i(\sigma/\omega\varepsilon_0)$ was added to take in account dc conductivity.

Table I summarizes the shape parameters found in the fitting procedure for each detected relaxation process.

In what concerns the fitting of the full polymerized mixture, the procedure was facilitated by the disappearance of the monomer's main relaxation [dashed line in Fig. 4(b)]. Figure 3(d), shows at −80 °C the secondary process of TrEGDMA followed by a secondary process of E7, that, by comparison between the 3D plots, Fig. 2(c) vs Fig. 2(a), is easily assigned to γ_{E7}, enhanced in the cured mixture. In Figs. 3(e) at −60 °C, the main process of the monomer is absent due to the cure and the main relaxation process of E7 appears. The gamma process is still observed in the medium frequency region. In Fig. 3(f) the three relaxation processes of E7: ε''_{slow}, $\varepsilon''_{\parallel}$ and $\varepsilon''_{\perp}$ are detected together with the remaining of the secondary relaxation of TrEGDMA. At higher temperatures, a MWS process was added due to the formation of a polymer matrix/liquid crystal interface, where the buildup of an interface polarization occurs. The fitting shape parameters used in the cured mixture are included in Table I. In the next lines the relaxation map presented in Fig. 4 is analyzed in more detail. As a first observation we can distinguish between Arrhenian and VFT behavior. Solid lines are the respective Arrhenian and VFT fittings, whose parameters are also summarized in Table I.

Whereas a linear activation plot is associated with localized relaxation processes, the non-Arrhenian behavior of the relaxation time of processes related with the glass transition reflects in the characteristic curvature of cooperative processes. Thus, the β secondary relaxation process associated to bulk TrEGDMA (crossed circles in Fig. 3) and γ from bulk E7 (crossed squares in Fig. 3) due to restricted mobility show Arrhenian behavior, while the processes associated to the main relaxation of both bulk materials have VFT behavior. Also both high and low frequency processes of bulk E7 present cooperative character, as denounced by previous data [14], nevertheless with less precision.

From Fig. 4(a) it can be seen that the relaxation times of the monomer main process detected in the precursor mixture is close to bulk TrEGDMA, showing a slight deviation to lower τ values, being absent when polymerization reached its completion [Fig. 4(b)]. On the other hand, the TrEGDMA secondary or β relaxation process persists after composite formation, with the same location than bulk TrEGDMA. The invariance in the frequency/temperature position of this secondary process was already found in previous results [15] independently of the monomer conversion degree. Its activation energy is equal, within the experimental error, for bulk, precursor and full polymerized mixture (Table I), having an average value of 36 ± 2 kJ mol^{-1}. The assignment of both main and secondary processes of TrEGDMA seems to be achieved.

In what concerns the main process of bulk E7, it can be observed from Fig. 4(b), that its relaxation times superimpose those of the main relaxation process found in the full polymerized mixture [open squares relatively to filled gray symbols in Fig. 4(b)]. A superposition of relaxation times is also observed for the high frequency process ($\varepsilon''_{\perp}$) in fully polymerized mixture relative to bulk E7 [slanted crossed squares relatively to filled gray symbols in Fig. 4(b)]. Thus, after PDLC formation, only the TrEGDMA's secondary relaxation process remains, confirming monomer conversion, while the liquid crystal maintains its bulk properties, as already observed in the DSC analysis. There are only intensity differences, since the equivalent electrical circuit for the composite system corresponds to a series association of two *RC* circuits, where the resultant resistance and capacitance are, respectively, higher and lower than the *RC* circuit that

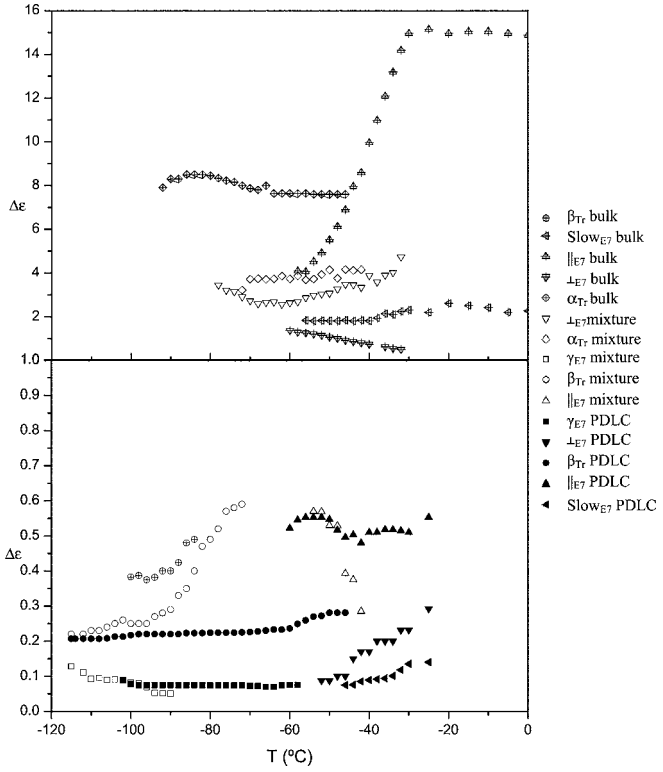

FIG. 5. Temperature dependence of the dielectric strength of the individual processes detected in precursor and full polymerized mixtures (see legend); data for bulk TrEGDMA taken from Ref. [15].

describes each bulk component, causing a significant depletion in the magnitude of the relaxation process. This magnitude can be quantified by the dielectric strength, $\Delta\varepsilon$, obtained throughout the fittings, whose temperature dependence is presented in Fig. 5. It is evident the intensity decrease for the liquid crystal processes detected in PDLC (full symbols) relatively to bulk E7 (crossed symbols in the upper part of Fig. 5 shown in a different scale).

Also the monomer's secondary relaxation (β_{Tr}) loses some intensity after polymerization compared with bulk TrEGDMA as shown in this figure (full against crossed circles). In what concerns the intensity differences between processes detected in bulk materials and precursor mixture, a decrease is also verified but to a lesser extent (crossed versus open symbols).

The question that remains is "What is happening to the liquid crystal in the initial mixture?" To help us to answer this question, Fig. 6 presents the isochronal plots at (a) 1 and (b) 100 kHz, taken from isothermal measurements, of all the intermediate conversion degrees measured at different t_{pol} (see Sec. II); the isochronal plots of bulk and full polymerized TrEGDMA taken from Ref. [15] are also included together with bulk E7.

The assignment of the first detected relaxation process in a temperature scale at 1 kHz raises no doubts: it is the secondary process of TrEGDMA, the only observable in bulk TrEGDMA after being polymerized at 120 °C. The alpha relaxation of the monomer is clearly distinguished in both isochronal plots, with a slight deviation to higher tempera-

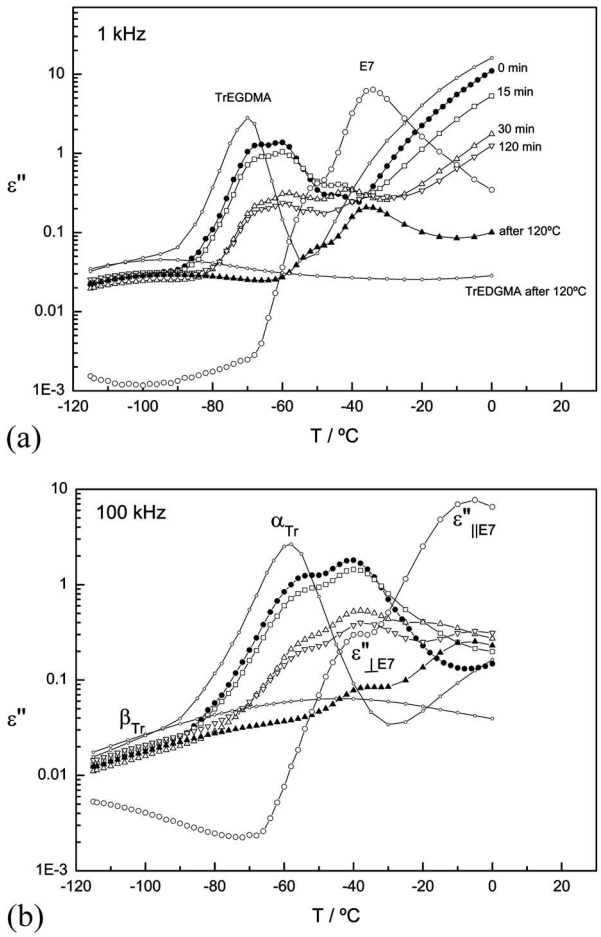

FIG. 6. Temperature dependence of dielectric loss at (a) 1 kHz and (b) 100 kHz for bulk constituents and all mixtures at different polymerization times [same symbols apply to both (a) and (b)].

tures in the starting mixture relative to bulk TrEGDMA, as the activation plot denounced by a small deviation to lower relaxation times [remember Fig. 4(a)]; this process masks the γ secondary relaxation of E7, perceived in the 1 kHz region [Fig. 6(a)] being absent in the loss data collected after the mixture being polymerized at 120 °C (full triangles).

In what concerns E7, the bulk behavior is reproduced, with lower intensity as already discussed, in the composite system after complete monomer conversion (full triangles). However, in the precursor mixture (full circles in Fig. 6) and for all intermediate polymerization times whenever monomer persists, the profile changes with the $\varepsilon''_{\perp}$ process enhanced relatively to the $\varepsilon''_{\|}$ relaxation that is highly suppressed in the mixtures at 0 and 15 min (open squares in Fig. 6), being merged under the tumbling mode process; the relative magnitude of the dielectric strength for these two processes in the precursor mixture (t=0 min) is shown in Fig. 5 [open down triangles in Fig. 5(a), $\Delta\varepsilon_{\perp}$ relative to open triangles in Fig. 5(b), $\Delta\varepsilon_{\|}$], being evident the more intense perpendicular process compared with the parallel that is decreasing until it is no more detectable. The position in the temperature axis of the $\varepsilon''_{\perp}$ process in the precursor mixture is significantly deviated to lower temperatures at 1 kHz relative to bulk E7, but is located at the same temperature posi-

tion at 100 kHz, denoting a change in the temperature dependence on the relaxation map of this process in the mixture in comparison with the pure liquid crystal; rather different activation plots were found for this tumbling mode in the starting mixture relatively to bulk E7 [slanted crossed squares relatively to filled gray squares in Fig. 4(a)].

V. DISCUSSION

Four relaxation processes were detected for bulk liquid crystal, however, with a poor definition in what concerns the gamma process. Both low and high frequency relaxation modes, respectively, $\varepsilon''_{\text{slow}}$ and $\varepsilon''_{\perp}$, are now better resolved relatively to previous results [14]. The behavior in the mixture after polymerization also allowed the detection of these processes together with the gamma relaxation, enhanced in the polymerized mixture, permitting a more precise dielectric characterization of the liquid crystal. From the VFT description of the temperature dependence of $\varepsilon''_{\parallel}$, $\varepsilon''_{\perp}$, and $\varepsilon''_{\text{slow}}$, nearly the same glass transition temperature is estimated, i.e., the extrapolation to $\tau=100$ s lead to almost a coincidence of all $\varepsilon''_{\parallel}$, $\varepsilon''_{\perp}$, and $\varepsilon''_{\text{slow}}$ VFT fittings, predicting, respectively, 207, 209, and 206 K, in a close agreement with the detected calorimetric glass transition temperature, 211 K.

The estimated fragility index for $\varepsilon''_{\parallel}$, $m=74$, is characteristic of fragile glass formers as the polyalchol threitol ($m=79$ [45]), *m*-toluidine ($m=79$ [46], 83 [47]) or the sidechain liquid crystalline polymer poly [3-(4′-cyanobiphenyloxy)propoxycarbonyl] ethylene ($m=74$ [48]) not being very far from the TrEGDMA monomer ($m=85$) [15].

In the precursor mixture the main changes are observed on the librational mode ($\varepsilon''_{\perp}$) of E7 that significantly deviates to lower temperatures/relaxation times [see Fig. 4(a)] which is an indication of higher mobility of the tumbling motion ($\varepsilon''_{\perp}$) in the precursor mixture. This, which also happens, to a less extent, with the process associated with the rotation around the short axis ($\varepsilon''_{\parallel}$), for mixtures from $t=0$ to $t=30$ min, when one compares with pure liquid crystal.

In bulk E7 the dielectric strength, $\Delta\varepsilon$, of $\varepsilon''_{\parallel}$ near 273 K is almost 30 times higher than that of $\varepsilon''_{\perp}$ (see Fig. 5), revealing that the dipole moment relaxes mainly through the parallel component. However, in TrEGDMA/E7 mixtures where polymerization didn't reach completion, the dielectric strength of both parallel and perpendicular components are comparable, with $\Delta\varepsilon$ for $\varepsilon''_{\perp}$ being even higher than for $\varepsilon''_{\parallel}$ in $t=0$ and $t=15$ min mixtures (see their peaks height in Fig. 6 and $\Delta\varepsilon$ in Fig. 5). The approximation in dielectric strength of the two processes is an indication of the increase of disorder of the liquid crystal molecules in the mixture, confirmed by the observation through: (i) polarized optical microscopy at room temperature, showing that the starting mixture is in the isotropic and homogeneous state and (ii) differential scanning calorimetry where the nematic to isotropic transition (clearing point) is absent (remember Fig. 1); the dielectric strength of the secondary gamma process for the liquid crystal is comparable between precursor and full polymerized mixture (full and open squares in Fig. 5).

A close inspection of Fig. 6(b) shows that while in the fully polymerized mixture (after 120 °C) the $\varepsilon''_{\parallel}$ relaxation has the same temperature location than bulk E7, in the mixture measured at $t_{\text{pol}}=30$ min (open triangles) it is deviated to lower temperatures, being completely merged under the $\varepsilon''_{\perp}$ relaxation at $t_{\text{pol}}=0$ and 15 min; whether this is a true coalescence between both processes or simply an effect resulting from the low intensity of the $\varepsilon''_{\parallel}$ relaxation is not clear. The merging is seen for frequencies above 3 kHz, i.e., not enough separation between the two processes exists at a significant range of frequencies to provide anisotropic behavior macroscopically. Figure 6(b), at 100 kHz, nicely illustrates the emerging of liquid crystal anisotropy and segregation of E7, i.e, encapsulation of the liquid crystal in the polymer matrix with the increase of polymerization time: initially the relaxation process of E7 is mainly a single peak as usual in the isotropic state and starts to split in two as t_{pol} increases, with further enhancement of $\varepsilon''_{\parallel}$ weight in the overall dielectric response relatively to $\varepsilon''_{\perp}$ accompanied by a depletion of the main relaxation process of the monomer. The coalescence of both processes at some frequencies is reflected in the small temperature range where reliable HN fittings are obtained in opposition to the large temperature interval found in the full polymerized mixture [open squares in Fig. 4(a) relatively to Fig. 4(b)] or bulk liquid crystal. As a consequence of the short temperature range where the $\varepsilon''_{\parallel}$ relaxation process is clearly detected the curvature is not well defined and thus the VFT parameters are affected by significant errors (see $\varepsilon''_{\parallel}$ precursor in Table I).

On the other side, in the initial mixture, the tumbling motion nearly follows the monomer behavior reflecting in a very close temperature dependence of relaxation times [crossed squares and open circles in Fig. 4(a)], that tend to coincide at low temperatures: the glass transition temperature estimated by VFT fittings is 188 K for both α_{Tr} and $\varepsilon''_{\perp}$ relaxations! This librational motion in the liquid crystal persists even after the short axis hindered rotations being frozen, that have higher glass transition. Even though that the motion around the long axis could originated a secondary glass transition, it will be impossible to differentiate it from the monomer's glass transition. However, making a parallelism with the δ relaxation occurring in liquid crystalline polymers which is mainly associated with the mobility modes of the longitudinal component of the dipolar moment of the mesogenic groups [49], the process is not active by DSC, because the changes in entropy are not sufficient to be translated into a significant change of heat capacity [50].

In what concerns the monomer's mobility, it suffers some hindrance in the mixture, opposite to what happens to the liquid crystal, as shown by a slight deviation to lower frequencies/higher temperatures of its relaxation loss peak relative to bulk. While TrEGDMA acts as a solvent relatively to E7, the monomer interacts with the liquid crystal molecules slowing down its dynamics, as usually happens in a mixture of components with different glass transitions. In polymer mixtures, if the constituents are completely miscible, a single glass transition should be detected obeying Fox equation [51], partial miscibility deviate each glass transition temperature towards the other component. In our mixture, the component, TrEGDMA, with lower T_g slightly increases its glass transition temperature (extrapolated dielectric VFT behavior for $\tau=100$ s: $T_{g\ \text{bulk}}=185$ K against

$T_{g\ \mathrm{mix}}=188$ K), while E7, with higher T_g, decrease it in a small amount (extrapolated dielectric VFT behavior of $\varepsilon''_{\parallel}$ for $\tau=100$ s $T_{g\ \mathrm{bulk}}=207$ K against $T_{g\ \mathrm{mix}}=204$ K) (see Table I).

The same conclusion can be drawn by observing the VFT plots in Fig. 4(a) of the main relaxation of both constituents that in the starting mixture, slightly deviates toward the other component relatively to bulk behavior. The calorimetric glass transitions (Fig. 1) suffered this slight increase/decrease of the glass transition temperatures of monomer/E7 of around 3 K. The initial mixture is thus phase separated in monomer and E7 rich phases, since some mutual solubility occurred between the two constituents. The partial solubilization of the monomer in a LC rich phase could prevent the mesomorphic order of this LC-rich phase being the reason why the nematic to isotropic transition is absent in the initial mixture, as suggested by a referee. By other side E7 is partially solubilized in the monomer rich phase. Nevertheless, the initial mixture is already phase separated as demonstrated by the calorimetric detection of the two T_g's and the dielectric detection of all the relaxation process characteristic of E7 and the monomer as well.

During the polymerization process the LC molecules are dissolved from the monomer rich phase. After full conversion, the system exhibits a behavior compatible with the segregation of the liquid crystal which is being encapsulated within the polymer matrix as revealed by the restore of E7's bulk characteristics and the disappearance of the monomer's main transition. The temperature dependences of the different relaxation times of the liquid crystal in the composite system overlap those of pure E7 and the calorimetric transitions match those of neat liquid crystal. The secondary relaxations of both constituents remain unaffected by mixing.

VI. CONCLUSIONS

A detailed characterization of pure nematic E7, starting mixture TrEGDMA/E7 60:40 w/w and polymerized composite were provided. The liquid crystal shows four different relaxation processes. A main process related with the parallel component of the dipole moment and two partially merged processes that appear as high and low frequency shoulders of the main process, related to, respectively, the perpendicular component of the dipole moment and a hindered mobility due to either molecular aggregates or partially immobilized molecules. The temperature dependence of the relaxation times of all these three processes show VFT behavior, as revealed in a previous work with less precision for the merged processes. A secondary process was detected for temperatures below 193 K that was enhanced in the starting mixture. The main changes in the molecular dynamics occur in the tumbling motion of the liquid crystal associated with the high frequency relaxation of the perpendicular component of the dipole moment. This process deviates significantly to higher/lower frequencies/temperatures being driven by the monomer's mobility. In the initial state the parallel component of the dipole moment relaxes highly superimposed to the perpendicular component in a significant range of frequencies resulting in a loss of macroscopic anisotropy. The monomer's dynamics, i.e., the lower T_g component slightly slows down due to some restriction imposed by interaction with the liquid crystal having a slightly higher T_g. In the polymerized mixture which was heated at 120 °C, the main relaxation of the monomer disappears and its secondary relaxation remains invariant. The liquid crystal relaxation processes restore their bulk mobility, confirming the monomer-liquid crystal segregation.

ACKNOWLEDGMENTS

The authors would like to acknowledge the financial support of Fundação para a Ciência e Tecnologia through Project Nos. POCTI/CTM/37435/2001, POCTI/CTM/47363/2002, and FEDER. M.T.V. and A.R.E.B. also thank Fundação para a Ciência e Tecnologia for Ph.D. Grant Nos. SFRH/BD/6661/2001 and SFRH/BD/23829/2005.

[1] M. Schadt, Annu. Rev. Mater. Sci. **27**, 305 (1997).
[2] J. W. Doane, *Liquid Crystals—Applications and Uses*, edited by B. Bahadur (World Scientific, Singapore, 1990), pp. 361–395.
[3] H. S. Kitzerow, Liq. Cryst. **16**, 1 (1994).
[4] P. S. Drzaic, *Liquid Crystals Dispersions* (World Scientific, Singapore, 1995).
[5] *Reflective Liquid Crystal Displays*, edited by S. T. Wu and D. K. Yang (Wiley, New York, 2001).
[6] S. K. Slimane, T. Bouchaour, M. Benmouna, A. Olivier, B. Carbonnier, T. Pakula, X. Coqueret, and U. Maschke, Mol. Cryst. Liq. Cryst. **413**, 1 (2004).
[7] R. Hasegawa, M. Sakamoto, and H. Sasaki, Appl. Spectrosc. **47**, 1386 (1993).
[8] J. E. Dietz and N. A. Peppas, Polymer **38**, 3767 (1997).
[9] K. S. Anseth, S. M. Newman, and C. N. Bowman, Adv. Polym. Sci. **122**, 177 (1995).
[10] *Radiation Curing in Polymer Science and Technology*, Volume IV: Practical Aspects and Applications, edited by J. P. Fouassier and J. F. Rabek (Elsevier, New York, 1993).
[11] M. T. Viciosa and M. Dionísio, J. Non-Cryst. Solids **341**, 60 (2004).
[12] Z. Z. Zhong, D. E. Schuele, W. L. Gordon, K. J. Adamic, and R. B. Akins, J. Polym. Sci., Part B: Polym. Phys. **30**, 1443 (1992).
[13] F. Roussel, J. M. Buisine, U. Mascchke, and X. Coqueret, Liq. Cryst. **24**, 555 (1998).
[14] M. T. Viciosa, A. M. Nunes, A. Fernandes, P. L. Almeida, M. H. Godinho, and M. Dionísio, Liq. Cryst. **29**, 429 (2002).
[15] M. T. Viciosa, C. M. Rodrigues, and M. Dionísio, J. Non-Cryst. Solids **351**, 14 (2005).
[16] J. M. Wacrenier, C. Druon, and D. Lippens, Mol. Phys. **43**, 97 (1981).
[17] D. Lippens, J. P. Parneix, and A. Chapoton, J. Phys. (Paris) **38**,

1465 (1977).
[18] Ch. Cramer, Th. Cramer, F. Kremer, and R. Stannarius, J. Chem. Phys. **106**, 3730 (1997).
[19] A. Schönhals and F. Kremer, *Molecular and Collective Dynamics of (Polymeric) Liquid Crystals In Broadband Dielectric Spectroscopy*, edited by F. Kremer and A. Schönhals (Springer, New York, 2002).
[20] G. P. Sinha and F. M. Aliev, Phys. Rev. E **58**, 2001 (1998).
[21] J. Leys, G. Sinha, C. Glorieux, and J. Thoen, Phys. Rev. E **71**, 051709 (2005).
[22] A. Drozd-Rzoska, S. Rzoska, S. Pawlus, and J. Ziolo, Phys. Rev. E **72**, 031501 (2005).
[23] M. Mierzwa, G. Floudas, and A. Wewerka, Phys. Rev. E **64**, 031703 (2001).
[24] G. Floudas, M. Mierzwa, and A. Schönhals, Phys. Rev. E **67**, 031705 (2003).
[25] J. F. Mano, N. T. Correia, and J. J. M. Ramos, Polymer **35**, 3561 (1994).
[26] D. Shenoy, S. Filipov, F. Aliev, P. Keller, D. Thomsen, and B. Ratna, Phys. Rev. E **62**, 8100 (2000).
[27] H. Hori, O. Urakawa, and K. Adachi, Macromolecules **37**, 1583 (2004).
[28] G. Williams, S. E. Shinton, and G. A. Aldridge, J. Polym. Sci., Polym. Phys. Ed. **39**, 1173 (2001).
[29] M. Boussoualem, F. Roussel, and M. Ismaili, Phys. Rev. E **69**, 031702 (2004).
[30] A. Miyamoto, H. Kikuchi, S. Kobayashi, Y. Morimura, and T. Kajiyama, Macromolecules **24**, 3915 (1991).
[31] M. Dionísio, Ana R. E. Brás, S. Henriques, T. Casimiro, A. Aguiar Ricardo, J. Sotomayor, J. Caldeira, and C. Santos, electronicLiquid Crystals, 2005/Mar/21.
[32] U. Maschke, M. Benmouna, and X. Coqueret, Macromol. Rapid Commun. **23**, 159 (2002).
[33] S. Havriliak and S. Negami, Polymer **8**, 161 (1967).
[34] H. Vogel, Phys. Z. **22**, 645 (1921).
[35] G. S. Fulcher, J. Am. Ceram. Soc. **8**, 339 (1925).
[36] G. Tammann and W. Hesse, Z. Anorg. Allg. Chem. **156**, 245 (1926).
[37] R. Bohmer, K. L. Ngai, C. A. Angell, and D. J. Plazek, J. Chem. Phys. **99**, 4201 (1993).
[38] G. W. Smith and N. A. Vaz, Liq. Cryst. **3**, 543 (1988).
[39] F. Roussel, J. M. Buisine, U. Maschke, and X. Coqueret, Mol. Cryst. Liq. Cryst. Sci. Technol., Sect. A **299**, 321 (1997).
[40] F. Roussel, U. Maschke, X. Coqueret, and J. M. Buisine, C. R. Acad. Sci., Ser. IIb Mec. Phys. Astron. **326**, 449 (1998).
[41] *Disorder Effects on Relaxational Processes*, edited by R. Richert and A. Blumen (Springer, Berlin, 1994).
[42] *Electricity and Magnetism*, edited by J. C. Maxwell (Clarendon, Oxford, 1892).
[43] R. W. Sillars, J. Inst. Electr. Eng. **80**, 378 (1937).
[44] K. W. Wagner, Arch. Elektrotech. (Berlin) **2**, 371 (1914).
[45] A. Döß, M. Paluch, H. Sillescu, and G. J. Hinze, Chem. Phys. **117**, 6582 (2002).
[46] C. A. Angell, J. Res. Natl. Inst. Stand. Technol. **102**, 171 (1997).
[47] N. Correia, C. Alvarez, J. J. Moura-Ramos, and M. J. Descamps, Chem. Phys. **113**, 3204 (2000).
[48] C. Alvarez and J. J. Moura-Ramos, Phys. Chem. Chem. Phys. **2**, 4743 (2000).
[49] M. Dionísio, N. M. Alves, and J. F. Mano, e-Polymers 044 (2004).
[50] J. F. Mano and J. L. Gómez Ribelles, Macromolecules **36**, 2816 (2003).
[51] T. G. Fox, Bull. Am. Phys. Soc. **1**, 123 (1956).